Neurobiology of Disease 125 (2019) 14–22

Contents lists available at ScienceDirect

Neurobiology of Disease

journal homepage: www.elsevier.com/locate/ynbdi

Brain insulin response and peripheral metabolic changes in a Tau transgenic mouse model

Antoine Leboucher[a,b,1], Tariq Ahmed[c,g,1], Emilie Caron[a,1], Anne Tailleux[d,1], Sylvie Raison[e], Aurélie Joly-Amado[f], Elodie Marciniak[a,b], Kevin Carvalho[a,b], Malika Hamdane[a,b], Kadiombo Bantubungi[d], Steve Lancel[d], Sabiha Eddarkaoui[a,b], Raphaelle Caillierez[a,b], Emmanuelle Vallez[d], Bart Staels[d], Didier Vieau[a,b], Detlef Balschun[c], Luc Buee[a,b,2], David Blum[a,b,*,2]

[a] Univ. Lille, Inserm, CHU Lille, UMR-S 1172 - JPArc, F-59000 Lille, France
[b] LabEx DISTALZ, F-59000 Lille, France
[c] Brain & Cognition, Faculty of Psychology & Educational Sciences, KU Leuven, Belgium
[d] Univ. Lille, Inserm, CHU Lille, Institut Pasteur de Lille, U1011- EGID, F-59000 Lille, France
[e] Institut des Neurosciences Cellulaires et Intégratives, Strasbourg, France
[f] Byrd Alzheimer's Institute, Department of Molecular Pharmacology and Physiology, University of South Florida, Tampa, FL, USA
[g] Neurological Disorders Research Center, Qatar Biomedical Research Institute, Hamad Bin Khalifa University, Doha, Qatar

ARTICLE INFO

Keywords:
Tau
Alzheimer's disease
Insulin resistance
THY-Tau22
Transgenic mice
Metabolism

ABSTRACT

Accumulation of hyper-phosphorylated and aggregated Tau proteins is a neuropathological hallmark of Alzheimer's Disease (AD) and Tauopathies. AD patient brains also exhibit insulin resistance. Whereas, under normal physiological conditions insulin signaling in the brain mediates plasticity and memory formation, it can also regulate peripheral energy homeostasis. Thus, in AD, brain insulin resistance affects both cognitive and metabolic changes described in these patients. While a role of Aβ oligomers and APOE4 towards the development of brain insulin resistance emerged, contribution of Tau pathology has been largely overlooked. Our recent data demonstrated that one of the physiological function of Tau is to sustain brain insulin signaling. We postulated that under pathological conditions, hyper-phosphorylated/aggregated Tau is likely to lose this function and to favor the development of brain insulin resistance. This hypothesis was substantiated by observations from patient brains with pure Tauopathies. To address the potential link between Tau pathology and brain insulin resistance, we have evaluated the brain response to insulin in a transgenic mouse model of AD-like Tau pathology (THY-Tau22). Using electrophysiological and biochemical evaluations, we surprisingly observed that, at a time when Tau pathology and cognitive deficits are overt and obvious, the hippocampus of THY-Tau22 mice exhibits enhanced response to insulin. In addition, we demonstrated that the ability of i.c.v. insulin to promote body weight loss is enhanced in THY-Tau22 mice. In line with this, THY-Tau22 mice exhibited a lower body weight gain, hypoleptinemia and hypoinsulinemia and finally a metabolic resistance to high-fat diet. The present data highlight that the brain of transgenic Tau mice exhibit enhanced brain response to insulin. Whether these observations are ascribed to the development of Tau pathology, and therefore relevant to human Tauopathies, or unexpectedly results from the Tau transgene overexpression is debatable and discussed.

1. Introduction

Alzheimer's disease (AD) is a neurodegenerative disorder characterized by the progressive development of memory deficits. AD is neuropathologically defined by extracellular accumulation of amyloid-β peptides into amyloid plaques and intraneuronal fibrillar aggregates of hyper- and abnormally phosphorylated Tau proteins (Masters et al., 1985; Sergeant et al., 2008). Tau pathology is observed early in the

* Corresponding author at: Inserm UMR_S1172, "Alzheimer & Tauopathies", Place de Verdun, 59045 Lille Cedex, France.
E-mail address: david.blum@inserm.fr (D. Blum).
[1] These authors equally contributed as first co-authors.
[2] These authors contributed as co-senior authors.

https://doi.org/10.1016/j.nbd.2019.01.008
Received 24 October 2018; Received in revised form 14 December 2018; Accepted 15 January 2019
Available online 19 January 2019
0969-9961/

brain stem and entorhinal cortex (Braak et al. 2011), and its progression in the cortex from entorhinal cortex, then hippocampus, and finally neocortex corresponds to the progression of the symptoms in AD (Duyckaerts et al., 1997; Grober et al., 1999; Nelson et al., 2012; Jucker and Walker, 2013).

In addition of these hallmarks, post-mortem brains from AD patients exhibit a reduced responsiveness to insulin, which is correlated with memory deficits (Talbot et al., 2012 and references herein). In accordance, analysis of neural origin-enriched plasma exosomes has shown an enrichment in pSer312-IRS-1 (associated with ineffective insulin signaling) in Alzheimer's disease patients (Kapogiannis et al., 2015; Mullins et al., 2017). Brain insulin resistance is thought to impair hippocampal plasticity and enhance cognitive deficits (see Gratuze et al., 2018 for review). Furthermore, it is also considered to favor the development of AD lesions themselves. Indeed, since insulin promotes the non-amyloidogenic processing of amyloid precursor protein (APP) (Pandini et al., 2013) and also increases expression of insulin-degrading enzyme (IDE; Zhao et al., 2004), insulin resistance is likely prone to favor the accumulation of amyloid-β. In addition, defective insulin signaling deregulates several kinases and phosphatases, favoring Tau hyperphosphorylation and aggregation (Gratuze et al., 2018 for review).

Molecular determinants of AD lesions would contribute themselves, in a vicious circle, to the development of brain insulin resistance. Several studies support the involvement of Aβ oligomers as a potential trigger for neuronal insulin resistance (Clarke et al., 2015; De Felice, 2013; Zhao et al., 2017; Bomfim et al., 2012 – but see however the results recently discussed by Stanley et al., 2016). A recent study from Zhao et al. (2017) also emphasized a role of ApoE4. In contrast, the role of Tau remains unclear. Intriguingly, Tau hyperphosphorylation results in the intraneuronal accumulation of insulin and in insulin signaling deficits (Rodriguez-Rodriguez et al., 2017). We have previously demonstrated that Tau physiologically favors brain insulin signaling, opening the possibility that a pathological loss of Tau function caused by its hyperphosphorylation and aggregation may promote brain insulin resistance (Marciniak et al., 2017). In line with this hypothesis, brain insulin resistance has been observed in post-mortem brains from patients with Tauopathies (Yarchoan et al., 2014). However, experimental proof of a link between Tau pathology and brain insulin resistance is lacking. In the present study, we addressed this question by evaluating the brain response to insulin in a transgenic mouse model of AD-like Tau pathology (THY-Tau22). Our data unexpectedly demonstrate that in THY-Tau22 mice, Tau pathology is associated with an increased response to insulin and peripheral metabolism changes, including resistance to high-fat diet.

2. Materials and methods

2.1. Animals

THY-Tau22 mice (C57BL6/J background) were generated by overexpression of human four-repeat Tau mutated at sites G272V and P301S under the control of Thy1.2 promoter (Burnouf et al., 2013; Schindowski et al., 2006; Van der Jeugd et al., 2013). Nontransgenic littermates (referred as WT) were used as age-matched controls. In all experiments, only males were used. All animals were maintained in standard animal cages under conventional laboratory conditions (12 h/12 h light/dark cycle, 22 °C), with ad libitum access to food and water. The animals were maintained in compliance with European standards for the care and use of laboratory animals and experimental protocols approved by the local Animal Ethical Committee (agreement APAFIS#2264-2015101320441671).

2.2. Hippocampal slices preparation

Mice were killed by cervical dislocation. Whole brains were rapidly removed from the skull and immersed for 1 min in ice-cold artificial cerebrospinal fluid (ACSF) solution containing (in mM): NaCl 117, KCl 4.7, $CaCl_2$ 2.5, $MgCl_2$ 1.2, NaH_2PO_4 1.2, $NaHCO_3$ 25 and glucose 10. The ACSF was continuously oxygenated with 95% O_2, 5% CO_2 to maintain the proper pH (7.4). The hippocampi were quickly removed and placed into ice-cold ACSF. Thereafter, transverse slices (400 µm thick) were prepared at 4 °C with a chopper (McIlwain Tissue Chopper, TC752). Slices were then placed in a holding chamber containing oxygenated ACSF, and kept at room temperature for at least 1 h before processing. Slices from THY-Tau22 mice were used either for electrophysiological recordings (see below) or for biochemical experiments. In the latter case, slices were treated 10 min with 200 nM insulin.

2.3. Electrophysiological recordings

Three to five slices were transferred into a custom-made submerged-type recording chamber and maintained at 32 °C constantly superfused with oxygenated ACSF (95% O_2, 5% CO_2) at a rate of 2.5 ml/min. After an incubation time of 90 min, field excitatory postsynaptic potentials (fEPSPs) were evoked in the stratum radiatum of the CA1-region by electrical stimulation of Schaffer collateral-commissural fibers using ACSF-filled glass micropipettes (2–5 MΩ). For stimulation, biphasic constant current square pulses (width 100 µs) were generated by an A-M Systems isolated pulse stimulator 2100 and delivered at a frequency of 0.033 Hz using a tungsten electrode (50 µm exposed tip). Signals were recorded and amplified with a 1700 differential amplifier (1700A, A-M Systems, bandpass filtered at 5 Hz and 10 kHz, respectively, and digitized using a CED 400 micro AD-converter (Cambridge Electronic Devices) and then further analyzed on-line by custom-made software. To analyze synaptic transmission efficiency, input/output curves were constructed by applying single stimuli in increments of 10 µA from 10 to 90 µA (data not shown). For subsequent experiments, the intensity of the stimulation was adjusted to elicit a fEPSP of 35% of the maximum and was kept constant throughout the experiment. In all experiments, baseline synaptic transmission was monitored for 30–60 min before drug administration. All values from the onset of insulin application until the end of recording were expressed relative to the control level (% of baseline).

2.4. Surgical procedures and injections

Bilateral cannulae (C235G-3.0/SPC with a removable dummy wire; Plastics One) were stereotaxically implanted into the lateral ventricles (coordinates with respect to Bregma: −0.7 mm anteroposterior [AP], +/− 1.5 mm mediolateral [ML], −2 mm dorsoventral [DV], according to the Paxinos and Franklin mouse brain atlas (2013) in anesthetized mice (1.5% isoflurane). Animals were allowed to recover for 1 week. The following 15 days, animals were habituated to the contention and injection procedure. Injections were performed in awake and freely moving mice. Animals were injected with 1 µl (per ventricle) of a solution containing either Vehicle (PBS, pH7.5) or Insulin (5 mg/mL) at the rate of 0.4 µL/min via cannula PE50 tubing (Plastics One) connected to a 10 µL Hamilton syringe pump system (KDS310; KD Scientific). The tubing was left in place for another 1 min at the end of each injection, and the cannula capped to prevent reflux of the injected solution. Placement of cannula was confirmed following post-mortem histology (not shown).

2.5. Biochemical analysis

For biochemical experiments, tissue was homogenized in 200 µL Tris buffer (pH 7.4) containing 10% sucrose and protease inhibitors (Complete; Roche Diagnostics GmbH), sonicated, and kept at −80 °C until use. Proteins from slices were extracted in RIPA buffer (Tris-HCl 10 mM; Sucrose 320 mM; NaCl 150 mM; NP40 1%; Sodium Deoxycholate 0.5%; SDS 0.1%; pH 8.0) for Western blot analysis from

slices. Protein amounts were evaluated using the BCA assay (Pierce), subsequently diluted with LDS 2× supplemented with reducing agents (Invitrogen), and then separated on NuPAGE Novex gels (Invitrogen). Proteins were transferred to nitrocellulose membranes, which were then saturated (5% non-fat dry milk or 5% BSA) in Tris 15 mmol/L (pH 8.0), NaCl 140 mmol/L, and 0.05% Tween and incubated with primary and secondary antibodies. Signals were visualized using chemiluminescence kits (ECL; Amersham Bioscience) and a LAS3000 imaging system (Fujifilm). Results were normalized to β-actin or GAPDH, and quantifications were performed using ImageJ software (Scion Software). Antibodies used for Western Blots were as follows: antibodies against Akt (#9272), pSer473-Akt (#9271), Insulin receptor β (#3025), IRS1 (#2382), pSer612IRS1 (#3203), PI3K-P85 (#4292), pY458-PI3K (#4228) were from Cell Signaling Technologies. pSer312IRS1 was from Thermofisher (18HCLC, ABfinity rabbit oligoclonal; 710,778). β-Actin was from Sigma-Aldrich (A5441) and GAPDH from Santa Cruz (FL-1-335). Anti-Total Tau was a homemade antibody (C-ter) recognizing the last 15 aa of COOH terminus.

2.6. mRNA extraction and quantitative real-time RT-PCR

Total RNAs were extracted from hippocampi and different peripheral organs of THY-Tau22 mice and purified using the RNeasy Lipid Tissue Mini Kit (Qiagen, Courtabœuf, France). One microgram of total RNA was reverse-transcribed using the High-Capacity cDNA reverse transcription kit (Applied Biosystem, Saint-Aubin, France). Quantitative real-time RT-PCR analysis was performed on an Applied Biosystems™ StepOnePlus™ Real-Time PCR Systems using TaqMan™ Gene Expression Master Mix (Life Technologies Corp., Grand Island, NY). The thermal cycler conditions were as follows: 95 °C for 10 min, then 40 cycles at 95 °C for 15 s and 60 °C for 1 min. Predesigned Taqman™ gene expression assays (Life Technologies Corp., Grand Island, NY) was used for human MAPT (Hs00213484_m1). Cyclophilin A (Mm02342430_g1) expression was assessed as a reference housekeeping gene for normalization. Amplifications were carried out in duplicates and the relative expression of target genes was determined by the ΔΔCt method.

Metabolic cages. Spontaneous feeding, respiratory exchange ratio and locomotor activity (total beam breaks/hour, X axis) were measured using metabolic cages (Phenomaster, TSE Systems, Germany). Briefly food intake and locomotor activity were monitored continuously for 24 h. Cumulative food intake was measured by the integration of weighing sensors fixed at the top of the cage from which the food containers were suspended into the home cage. Locomotor activity was assessed using a metal frame placed around the cage. Evenly spaced infrared light beams are emitted along X axis. Beam interruptions caused by movements of the animals are sensed and registered at high resolution. The sensors for detection of movement operate efficiently under both light and dark phases, allowing continuous recording. Mice were housed individually and acclimated to the home cage for 72 h prior experimental measurements.

2.7. Evaluation of circadian changes

Animals were housed in individual cages with running wheels. Mice were bred within a pathogen-free animal care facility (Chronobiotron platform, UMS 3415, CNRS and University of Strasbourg) in a 12:12-hour light/dark (LD) cycle, with lights on (07.00 h), at 22 ± 1 °C and 55 ± 5% humidity. Food and tap water were provided ad lib. Wheel running activity was recorded in LD during 20 days, before transferring and recording wheel running activity in constant darkness (DD) condition. Daily rhythms of wheel-running activity under LD were analyzed with ClockLab software (Actimetrics, Evanston, IL, USA) using the 'Activity profile' function. In constant darkness (DD), endogenous period (T) were calculated using, the 'Periodogram' functions of ClockLab.

2.8. High fat diet

THY-Tau22 mice and WT littermates were fed with CHOW diet (RM1A, Special Diets Services, Essex, Great Britain) or High-Fat Diet (HFD, H; 59% kCal from fat; Ssniff, D12331) from 4 months of age. Animals of each genotype were assigned to balanced groups according to their initial body weight. Body weights were measured weekly. At completion of the experiment (i.e. following 20w of diet), mice were about 9 month-old.

2.9. Biochemical plasma parameter

Plasma was collected at the tail vein after a 6-h fasting, and parameters were determined as follows: blood glucose (Accu-Chek Performa glucometer; Roche Diagnostics GmbH); plasma insulin and leptin measured, respectively, using ultrasensitive insulin ELISA (Mercodia AB), and mouse/rat leptin enzyme immunoassay kit (Spibio). Total and HDL-cholesterol as well as triglycerides were measured by enzymatic method using ready-to-use kits (Biomérieux).

2.10. Glucose tolerance tests

Glucose tolerance (IPGTT) was assessed following a 6-h fast. D(+) glucose (1 g/kg; Sigma-Aldrich) was injected intraperitoneally. Blood glucose was then measured at 0, 15, 30, 60, 90, and 120 min following injection.

2.11. Statistics

Results are expressed as mean ± SEM. Statistics were performed using either Student's *t*-test as well as One or Two-way analysis of variance (ANOVA), followed by a post-hoc Fisher's LSD test using Graphpad Prism Software. P values $< .05$ were considered significant.

3. Results

3.1. Enhanced brain response to insulin in THY-Tau22 mice

In order to evaluate whether brains of mice developing AD-like Tau pathology exhibit impaired responsiveness to insulin, we used hippocampal slices from THY-Tau22 mice, which overexpress a pro-aggregative mutated (G272V/P301S) 1N4R human Tau protein (Schindowski et al., 2006) under the control of a neuronal promoter (Thy1.2). Animals were tested at 8–10 months of age, when they exhibit memory deficits, without neuronal loss (Burnouf et al., 2013; Van der Jeugd et al., 2013). We evaluated insulin-induced hippocampal long-term depression of extracellular field excitatory postsynaptic potentials (LTD; Van der Heide et al., 2005; Marciniak et al., 2017) by incubation of insulin for 30 min with a low insulin concentration (500 nM). As shown in Fig. 1A, in these conditions, WT mice displayed a small depression of recordings by 15.0 ± 2.8% compared with baseline (240 min: $p = .0024$, One-sample *t*-test). Conversely, in THY-Tau22 mice, the magnitude of LTD was significantly greater (at 240 min, THY-Tau22: 39.6 ± 7.4%, WT: 15.0 ± 2.8%; $p = .012$ vs WT, Student's t-test; 1-240 min $p < .01$, Two Way (RM)-ANOVA). The greater magnitude of insulin responsiveness of THY-Tau22 hippocampal tissue was confirmed in another set of experiments that revealed significantly enhanced Akt ex-vivo phosphorylation in THY-Tau22 (8-10 m old) slices as compared to slices of littermate controls upon insulin treatment (Fig. 1B). Noteworthy, as reported earlier (Troquier et al., 2012; Leboucher et al., 2013; Laurent et al., 2016, 2017), hippocampal slices from 8 to 10 m-old THY-Tau22 mice exhibit Tau pathology (not shown).

Next, we addressed the known effect of intracerebroventricularly-administered insulin (bilateral icv injection in lateral ventricles) to reduce body weight gain (Brown et al., 2006; Woods et al., 1979) in 8 m-

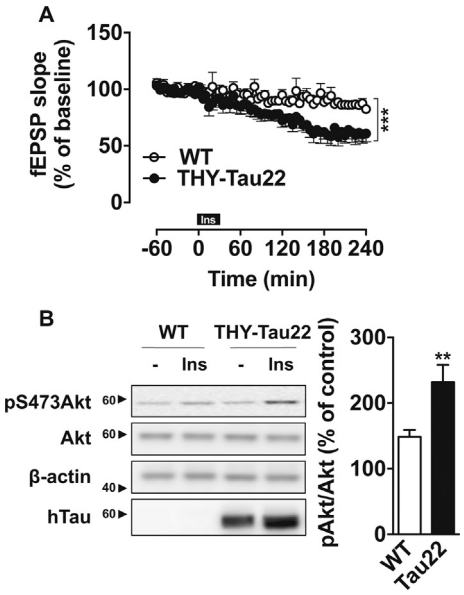

Fig. 1. Enhanced response to insulin in the hippocampus of THY-Tau22 mice. **(A)** Long-term depression induced by insulin (500 nM, 30 min, see bar labeled ins) in the hippocampal CA1-region of THY-Tau22 mice and littermate controls. Each point represents mean ± SEM normalized to baseline values preceding the application of insulin (n = 7–8/group; ***p < .001, RM Two-Way ANOVA. **(B)** Akt phosphorylation in hippocampal slices from THY-Tau22 mice and controls, 10 min following insulin treatment (200nM; n = 9/group, **p < .01, Student's t-test). Results are expressed as means ± SEM. Controls are indicated as open circles/bars, transgenic animals as black circle/bars. WT and THY-Tau22 mice were 8-10 m-old.

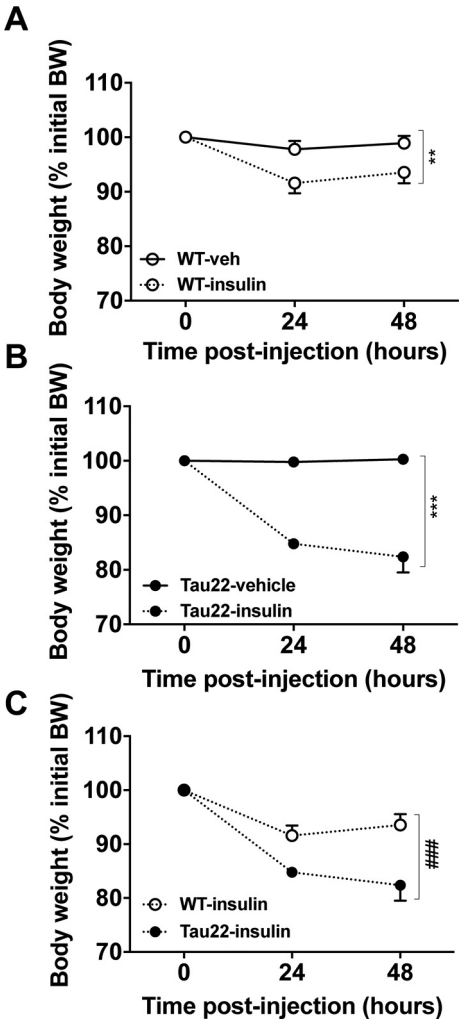

Fig. 2. Effect of brain insulin administration on body weight in WT and THY-Tau22 mice. WT **(A)** and THY-Tau22 **(B)** body weights were measured 24h and 48 h following intracerebroventricular injection of PBS or insulin (2μL, 5 mg/mL; n = 3–4/group; **p < .01; ***p < .001 vs. PBS injected animals; ### p < .001 vs. WT animals injected with insulin; Two-Way ANOVA). Comparison between WT and THY-Tau22 mice injected with insulin is shown in **(C)**. Results are expressed as mean percentage ± SEM of initial respective body weight. WT mice are indicated as open circles, THY-Tau22 mice as black circles. WT and THY-Tau22 mice were 8 m-old.

old THY-Tau22 mice and littermate controls. As expected, icv insulin was able to promote body weight loss in WT mice (Fig. 2A; p < .01 vs. Veh, using Two-Way ANOVA) and THY-Tau22 mice (Fig. 2B; p < .001 vs. Veh, using Two-Way ANOVA). We estimated that the cumulated food intake during this 48 h period dropped by 46.1 ± 7.6%, in line with the data we previously published for control animals (Marciniak et al., 2017). Interestingly, body-weight loss induced by icv insulin was significantly greater in THY-Tau22 mice as compared to WT littermates (Fig. 2C; p < .001 vs. WT, using Two-Way ANOVA), in line with 78.1 ± 6.9% drop of food intake estimated during the same 48 h period (p = .029 vs. WT using Student's t-test). Noteworthy, above-mentioned modifications in the response to exogenous insulin was not linked to changes in the basal insulin signaling in the brain of THY-Tau22 mice as compared to controls (Fig. S1). Altogether, these data indicated that brain response to insulin is enhanced in Tau transgenic mice.

3.2. Enhanced response to brain insulin is associated with metabolic changes in THY-Tau22 mice

Both genetic deletion of neuronal insulin receptors and hypothalamic insulin receptor knock-down have been previously shown to increase food intake, body weight gain and adiposity in rodents (Brüning et al., 2000; Grillo et al., 2007; Obici et al., 2002; Gratuze et al., 2018 for review). In accordance with an enhanced insulin response in the brain of THY-Tau22 mice, we found, using metabolic cages, that 10-11 m-old Tau transgenic mice exhibited a reduced basal food intake when fed ad libitum (Fig. 3A), associated with an increased locomotor activity (Fig. 3C). Respiratory exchange ratio (RER) remained unaltered suggesting no change of energy substrate oxidation at the tissue level (Fig. 3B). According to the difference observed in term of response to icv insulin and metabolic cages experiments, body weight gain was significantly reduced in THY-Tau22 mice as compared with WT littermates (Fig. 4B) in absence of body weight change at weaning (Fig. 4A).

Adiposity was significantly reduced in THY-Tau22 mice as exemplified by reduced circulating leptin levels (Fig. 4C), decreased adipose tissue leptin mRNA expression (Fig. 4D) and reduced adipose tissue (Fig. 4E–F) at the age of 10-12 m. Importantly, while glycemia remained unchanged (Fig. 4H), THY-Tau22 mice displayed a significantly reduced insulinemia (Fig. 4I). Also, while IPGTT profile remained similar, insulin levels measured 15 min following glucose injection were found lower in THY-Tau22 mice compared to WT littermates (Fig. 4J). Finally, triglycerides, cholesterol and HDL-cholesterol plasma levels were reduced in THY-Tau22 mice (Fig. 4K–M). Circadian functions impact on peripheral metabolism (Gachon et al., 2017) and impaired normal circadian clock function has been described in Tau transgenic mice (rTg4510; Stevanovic et al., 2017). As shown on Fig. S2A, and in line with locomotor activity (Fig. 3C), wheel running activity recorded in a 12:12-hour light/dark cycle was found higher during the dark phase in THY-Tau22 (p < .0001 vs WT Littermates, Two-Way ANOVA). Wheel-running activity rhythms of WT and THY-Tau22 transgenic mice were synchronized on the light–dark cycle and free-ran under constant darkness (DD) conditions (Fig. S2C–D). The endogenous

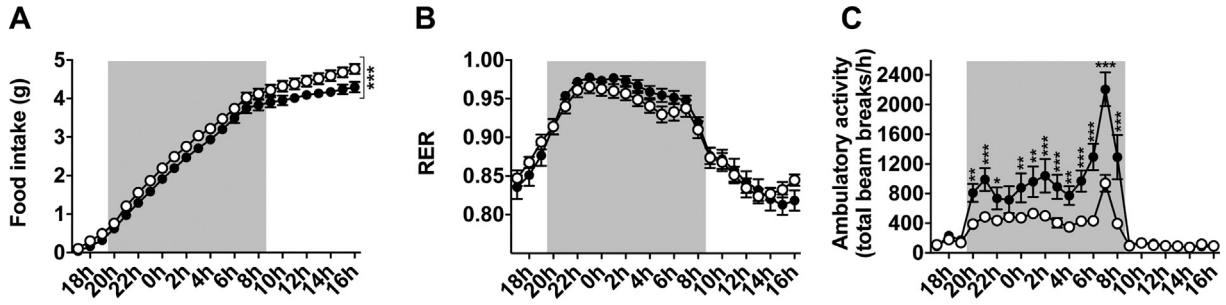

Fig. 3. Evaluation of food intake, respiratory exchange ratio and ambulatory activity in WT and THY-Tau22 mice. Tau overexpression in mice is associated with hypophagia and nocturnal hyperactivity. **(A)** 24h-cumulative food intake (g) of Tau22 (black circles) and control (white circles) littermates fed with a chow diet (*** $p < .001$ vs WT; two-way ANOVA). **(B)** 24h-respiratory exchange ratio (RER = VCO2/VO2) in Tau22 (black circles) and control (white circles) littermates. **(C)** 24h-spontaneous locomotor activity (total beam breaks/h) in Tau22 (black circles) and control (white circles) littermates (n = 14–16/group; *$p < .05$, **$p < .01$, ***: $p < .001$; two-way ANOVA followed by Fisher's LSD post-hoc test). Results are expressed as mean ± SEM. WT mice are indicated as open circles, THY-Tau22 mice as black circles. WT and THY-Tau22 mice were 8-10 m-old.

period calculated in DD was not significantly different between mice being close to 23.8 h and 24 h respectively (Fig. S2B). Finally, metabolic changes of THY-Tau22 mice were apparently ascribed to central/neuronal changes since human Tau transgene expression, driven by Thy1.2 promoter was, as expected, strongly detected in the brain but not in peripheral tissues (Fig. S3), in accordance with previous observations (Laurent et al., 2017). Noteworthy, skeletal muscle tissue displays hTau mRNA expression of about 1% of the hippocampal expression.

Considering the metabolic changes associated with human Tau overexpression in THY-Tau22 mice observed under Chow diet (Fig. 4), we challenged WT and THY-Tau22 transgenic mice with high-fat diet (HFD; Fig. 5). Ten to twelve mice of each genotype were fed with Chow or HFD diets, starting at 4 months until 9 months of age. Although WT mice progressively developed obesity under HFD ($p < .001$, using Two-Way ANOVA), reaching, at completion of the experiment, 36.4 ± 5.9% above the initial body weight, THY-Tau22 mice exhibited a significantly reduced body weight gain under HFD (24.9 ± 3.6% of the initial body weight, $p < .001$; WT HFD vs. THY-Tau22 HFD, using Two-Way ANOVA; Fig. 5A). Accordingly, at completion of the HFD regimen, THY-Tau22 exhibited a significant reduction of circulating leptin (Fig. 5B), white adipose tissue mass (Fig. 5C–D) as well as plasma cholesterol and HDL-cholesterol (Fig. 5G–H). HFD feeding led to a significant increase in fasting glycemia and insulinemia in WT mice that were however significantly lower in THY-Tau22 mice as compared to WT littermates (Fig. 5I–J). Interestingly, while IPGTT profiles were markedly and similarly impaired by the HFD in both WT and THY-Tau22 mice ($p < .001$ vs. respective Chow groups, using Two-Way ANOVA; Fig. 5K–L), THY-Tau22 transgenic mice exhibited significantly lower insulin levels 15 min following glucose injection under HFD (Fig. 5M), together with a significantly reduced HOMA index (WT Chow:5.7 ± 1.7; WT HFD:36.7 ± 6.7; THY-Tau22 Chow:3.4 ± 0.6; THY-Tau22 HFD: 14.1 ± 2.0; WT Chow vs. WT HFD: $p < .001$; THY-Tau22 Chow vs. THY-Tau22 HFD: $p < .05$; WT HFD vs. THY-Tau22 HFD: $p < .001$) suggesting that THY-Tau22 mice exhibit higher insulin sensitivity as compared to WT animals.

4. Discussion

Brains of patients with Alzheimer's disease have been reported to exhibit an insulin-resistance state, the so-called “type 3 diabetes” (de la Monte, 2014) characterized by significant impairments of insulin signaling and related pathways (Moloney et al., 2010; Talbot et al., 2012; Rodriguez-Rodriguez et al., 2017) which is thought to contribute to memory decline (Grillo et al., 2015; Benedict and De Felice, 2015). So far, while previous data emphasize a role for Aβ oligomers (Zhao et al., 2017; Gratuze et al., 2018 for review) and ApoE4 (Zhao et al., 2017), the contribution of Tau pathology remains poorly understood.

In this study, we report that THY-Tau22 mice, overexpressing a mutated human Tau protein, display an increased brain response to insulin. First, we show that hippocampal slices from THY-Tau22 mice challenged with exogenous insulin exhibit an enhanced insulin-induced hippocampal long-term depression and Akt phosphorylation when compared to WT littermates. Second, increased brain insulin sensitivity was also evidenced by an increased body weight loss following insulin i.c.v. injection in THY-Tau22 mice as compared to WT. Overall, these data suggest that THY-Tau22 mice exhibit a higher brain response to insulin.

Brain insulin signaling is known to play an important role in the regulation of peripheral glucose metabolism and energy homeostasis. For instance, in rodents, both genetic deletion of neuronal insulin receptors (NIRKO mice) and hypothalamic knock-down of insulin receptors were previously shown to increase food intake and body weight gain as well as to favor insulin resistance, hyperinsulinaemia and hypertriglyceridaemia (Brüning et al., 2000; Obici et al., 2002; Grillo et al., 2007). The basal metabolic changes observed in our Tau transgenic mice, such as lower body weight -presumably related to decreased food intake and increased locomotor activity-, decreased leptin and reduced adipose tissue were therefore in accordance with the known regulatory impact of central insulin signaling upon peripheral metabolism.

In line with the basal metabolic phenotype of THY-Tau22 mice, we also demonstrated their resistance to high-fat diet. Diet-induced obesity leads to metabolic syndrome i.e. hyperinsulinemia, hypertriglyceridemia, glucose intolerance and insulin resistance. When we challenged our THY-Tau22 mice with high-fat diet, they showed a different response than WT littermates. Under high-fat diet, both THY-Tau22 and WT gained weight, although THY-Tau22 to a lesser extent. As expected, weight gain in WT animals resulted in increased adipose tissue mass, together with hypertriglyceridemia, hyperleptinemia, hyperglycemia and hyperinsulinemia that led to glucose intolerance, all signs of the metabolic syndrome. Interestingly, even if THY-Tau22 mice displayed hypertriglyceridemia and high cholesterol under high-fat-diet, in contrast to WT mice, this excess in fat did not convert into an increase in adipose tissue content. Moreover, under high-fat diet, Tau transgenic mice remained hypoleptinemic and hypoinsulinemic compared to WT littermates. These results are similar to the phenotype observed in different mouse models of Alzheimer's disease. Indeed, Tg4510 mice, that accumulate Tau in the forebrain, exhibit body weight loss, decreased adipose tissue and hypoleptinemia (Joly-Amado et al., 2016). In Tg2576, a model of amyloid deposition, decreased body weight and adipose tissue together with low leptin levels were also noticed even before accumulation of amyloid plaques (Ishii et al., 2014). In addition, although THY-Tau22 and WT mice displayed glucose intolerance to the same extent, insulin levels 15 min were significantly lower following glucose challenge under HFD in THY-Tau22 which also exhibited significantly reduced HOMA-IR suggesting that THY-Tau22 were

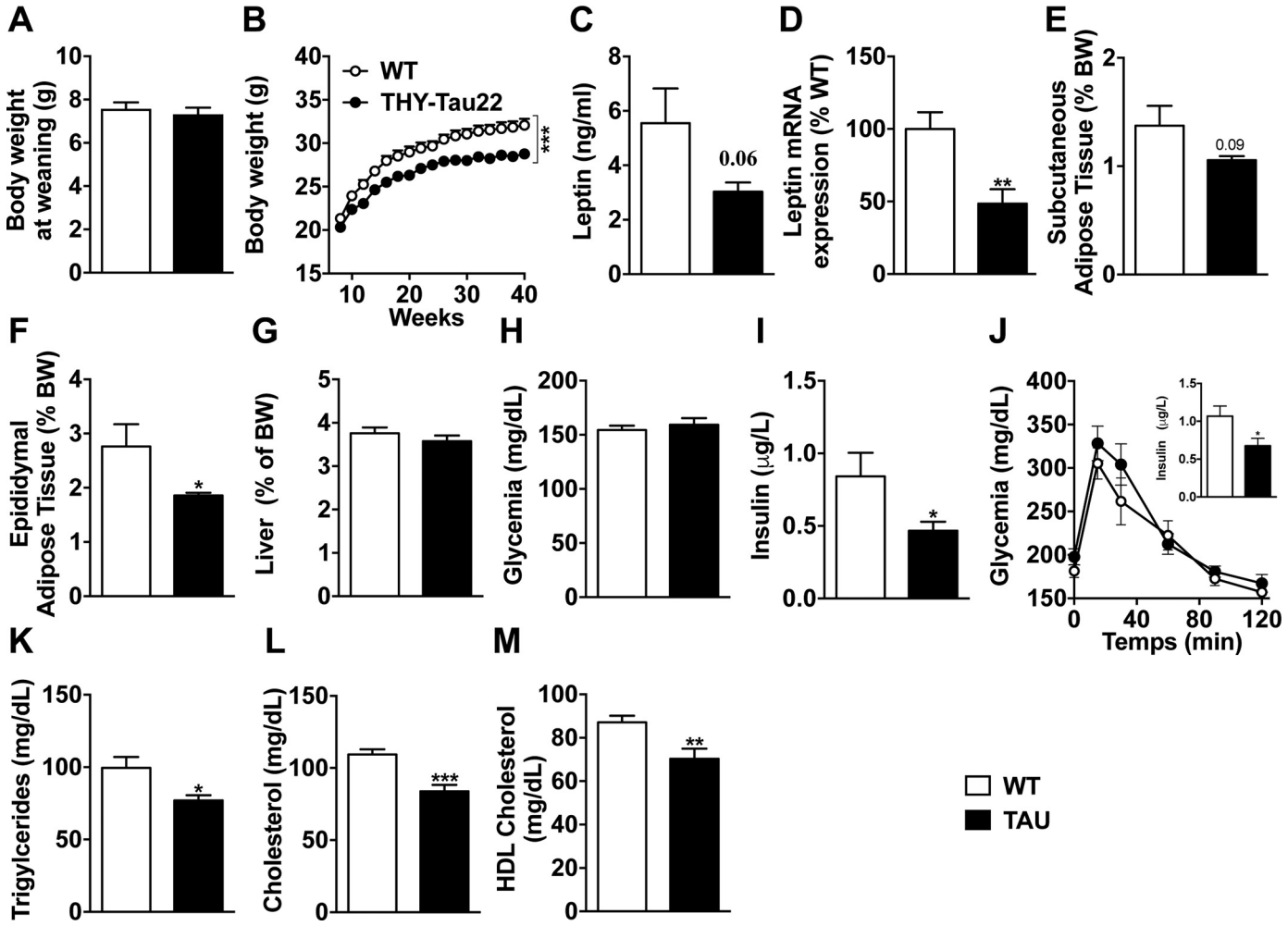

Fig. 4. Metabolic phenotyping of THY-Tau22 mice. (A) Body weight at weaning (n = 11–13/group; NS, Student's t-test); **(B)** Body weight gain (n = 11–12/group; ***p < .001, Two-Way ANOVA); **(C)** Plasma leptin (n = 14–16/group; p = .06, Mann-Whithney); **(D)** mRNA expression of leptin by white adipose tissue (n = 5–7/group; **p < .01, Student's t-test); **(*E*-F)** Subcutaneous and epididymal adipose tissue weight (n = 10–11/group; *p < .05, Student's t-test); **(G)** Liver weight (n = 10–11/group, NS); **(H)** Glycemia (n = 10–11/group); **(I)** Insulinemia (14–15/group; *p < .05 Student's t-test); **(J)** Glucose tolerance (n = 8/group). Inset represents plasma insulin levels 15 min after glucose injection (*p < .05 usinf Student's t-test); **(K-M)** Plasma triglycerides, total cholesterol and HDL cholesterol (n = 10–11/group, *p < .05, **p < .01, ***p < .001, Student's t-test). Results are expressed as mean ± SEM. WT mice are indicated as open circles/bars, THY-Tau22 mice as black circles/bars. WT and THY-Tau22 mice were 10-12 m-old.

somewhat protected against high-fat diet-induced insulin resistance. Together, brain insulin response and the associated peripheral metabolic phenotype of THY-Tau22 mice clearly demonstrate that, unexpectedly, our Tau transgenic mouse model does not develop the central insulin resistance previously reported in the brain of patients with Tauopathies (Yarchoan et al., 2014).

Importantly, recent studies, including ours, have demonstrated that constitutive Tau knock-out mice exhibit a reduced brain response to insulin as well as enhanced food intake and body weight gain along with increased adiposity and glucose homeostasis impairments (Marciniak et al., 2017; Wijesekara et al., 2018), a phenotype which obviously mirrors the present changes observed in THY-Tau22 mice. Interestingly, Tau was found to be expressed in the pancreatic islets and metabolic changes were suggested to arise from a reduction of insulin content and impaired glucose-stimulated insulin secretion (Wijesekara et al., 2018). In THY-Tau22 mice, the human Tau transgene was found strongly expressed in the brain of THY-Tau22 mice but mostly not in peripheral organs. This is in line with previous data, demonstrating that the Thy1.2 expression cassette drives expression solely in neurons (Vidal et al., 1990; Caroni, 1997; Laurent et al., 2017). It is therefore likely that the peripheral phenotype, notably the changes in glucose homeostasis of THY-Tau22 mice, is a consequence of central-based regulations. However, it is noteworthy that skeletal muscle of THY-Tau22 mice exhibit a very low but not null mRNA expression of hTau transgene. Considering our previous data showing that Tau reduces PTEN activity (Marciniak et al., 2017), thereby favoring insulin signaling and given that muscle-specific PTEN has been shown to increases insulin sensitivity and protect from high-fat induced insulin-resistance (Wijesekara et al., 2005), we cannot firmly rule out that a small amount of human Tau in myocytes would also contribute, by inhibiting PTEN, to the metabolic phenotype observed in THY-Tau22 mice. This will deserve further investigations. Glucose homeostasis and peripheral metabolism are notably regulated by the hypothalamus, in particular through changes in autonomic nervous system output. For instance, sympathetic and parasympathetic fibers which richly innervate pancreatic beta cells play an important role in insulin secretion. Activation of the sympathetic nervous system decreases insulin plasma levels (Bloom et al., 1975; Sharp, 1996). In adipose tissue, sympathetic system stimulation reduces leptin gene expression (Trayhurn et al., 1995) and plasma concentration (Bing et al., 1998) whereas it increases lipolysis (Steiner et al., 1985), thus limiting lipids storage (Randle et al., 1963). Interestingly, although we did not assess directly hypothalamic insulin sensitivity in THY-Tau22 mice, they exhibit hypoinsulinemia, hypoleptinemia, decreased leptin gene expression as well as reduced fat

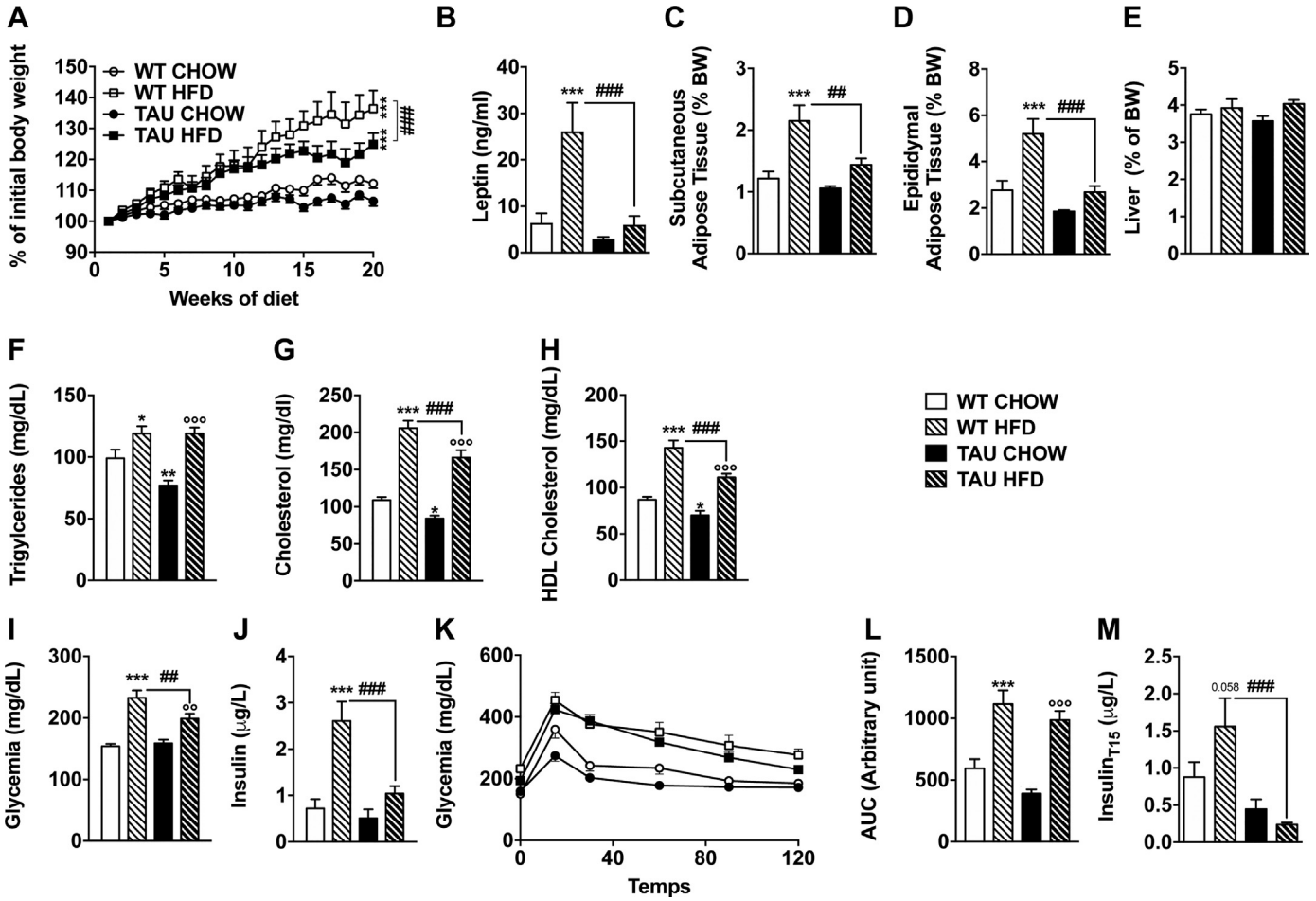

Fig. 5. Metabolic phenotyping of WT and THY-Tau22 mice under HFD. (A) Body weight gain of WT and THY-Tau22 mice under HFD given from 4 to 9m of age (n = 10–11/group; ***p < .001 vs respective Chow control; ###p < .001 WT HFD vs. THY-Tau22 HFD, Two-Way ANOVA); **(B)** Plasma leptin (n = 8–11/group; ***p < .001 vs WT Chow, ###p < .001 WT HFD vs. THY-Tau22 HFD, One-Way ANOVA followed by LSD Fisher post-hoc test); **(C-D)** Subcutaneous and epididymal adipose tissue weight (n = 10–12/group; ***p < .001 vs WT Chow, ##p < .01 & ###p < .001 WT HFD vs. THY-Tau22 HFD, One-Way ANOVA followed by LSD Fisher post-hoc test); **(E)** Liver weight (n = 10–12/group, NS); **(F–H)** Plasma triglycerides, total cholesterol and HDL cholesterol (n = 10–12/group; *p < .05, **p < .01 & ***p < .001 vs WT Chow, °°°p < .001 vs THY-Tau22 Chow, ###p < .001 WT HFD vs. THY-Tau22 HFD, One-Way ANOVA followed by LSD Fisher post-hoc test); **(I)** Glycemia (n = 10–12/group; ***p < .001 vs WT Chow, °°p < .01 vs THY-Tau22 Chow, ##p < .01 WT HFD vs. THY-Tau22 HFD, One-Way ANOVA followed by LSD Fisher post-hoc test); **(J)** Insulinemia (n = 9–12/group; ***p < .001 vs WT Chow, ###p < .001 WT HFD vs. THY-Tau22 HFD, One-Way ANOVA followed by LSD Fisher post-hoc test); **(K)** Glucose tolerance (n = 9–11/group) and **(L)** related AUC (n = 9–11/group; ***p < .001 vs WT Chow, °°°p < .001 vs THY-Tau22 Chow, One-Way ANOVA followed by LSD Fisher post-hoc test). **(M)** Plasma insulin levels 15 min after glucose injection (n = 7–9/group; ###p < .001 WT HFD vs. THY-Tau22 HFD, One-Way ANOVA followed by LSD Fisher post-hoc test). Results are expressed as mean ± SEM. WT mice are indicated as open circles/bars, THY-Tau22 mice as black circles/bars. HFD groups are represented by squares or dashed bars. WT and THY-Tau22 mice were treated with HFD from 4 to 9 m of age.

mass. This suggests that mutant mice present hypothalamic alterations that have already been described in AD patients (reviewed in Gratuze et al., 2018).

The brain resistance to the effect of exogenous insulin that we previously observed in Tau knock-out mice (Marciniak et al., 2017) is diametrically opposed to the present THY-Tau22 data. Indeed, we report here that THY-Tau22 mice exhibit a higher electrophysiological and biochemical response to exogenous insulin (Fig. 1) while we described that Tau KO mice display a blunted response to exogenous insulin (Marciniak et al., 2017). Further, we report in the present study that THY-Tau22 exhibit a lower food intake, increased locomotor activity, reduced body weight gain, hypoleptinemia, hypoinsulinemia and improved glucose tolerance (Fig. 4) while, in sharp contrast, Tau KO mice exhibit increased food intake, lower locomotor activity, higher body weight gain, higher leptinemia, higher insulinemia and glucose intolerance (Marciniak et al., 2017; Wijesekara et al., 2018). Therefore, opposite results are obtained from a loss of function model (Tau KO) and a transgenic Tau model. In a pathophysiological situation, when Tau aggregates, it is relevant to think that neurons experience simultaneously a toxic gain of function due to Tau oligomerization/aggregation and a detrimental loss of Tau physiological functions, leading to neuronal dysfunction and death. While this deserve future studies in knock-in tau models, pathological loss of Tau function would be therefore prone to favor brain insulin resistance. In Tau transgenic models overexpressing human mutated Tau prone to aggregate, we cannot unfortunately exclude that some phenotypes like the ones observed in the present study may rather relate to Tau overexpression itself, representing a gain of Tau function, irrelevant to the pathology but rather related to the physiological function of Tau. Indeed, when referring to previous data from our laboratory, only a part of the overexpressed human mutated Tau (50–60%) is present as sarkosyl-insoluble in hippocampal fractions (Troquier et al., 2012; Leboucher et al., 2013), with a non-negligible part of overexpressed Tau remaining soluble. Considering that the sole human WT Tau overexpression in neuroblastoma cells, which remains in a soluble state, is prone to confer insulin-sensitivity to neuroblastoma cells (Marciniak et al., 2017),

recapitulating the enhanced response to insulin as seen in the hippocampus of THY-Tau22 transgenic mice, one may consider that the brain insulin sensitivity observed in THY-Tau22 model could be the consequence of the presence of high amount of soluble human Tau protein in neurons and not the consequence of Tau pathology itself. This makes sense if one considers that overexpressed Tau protein is prone to bind and inhibit PTEN phosphatase, a negative regulator of insulin signaling (Marciniak et al., 2017). From that point-of-view, the THY-Tau22 model would therefore not fully recapitulate the pathological loss-of-Tau function taking place in the brain of patients with AD or Tauopathies, and, the phenotypes observed in our study could be considered as the eventual artefactual consequences of the accumulation of soluble Tau in transgenic THY-Tau22 mice. Finally, it is also important to mention that while Yarchoan et al. (2014) reported a slight but significant increase in serine phosphorylation of IRS-1 in pure Tauopathies, it was found actually much higher in patients with AD. These data may either suggest that either Aβ oligomers or the combined presence of both Aβ and Tau pathology have more potency than Tau pathology alone to promote IRS-1 dysregulation. In this context, a major inhibition of insulin signaling by Tau pathology would not be expected in a Tau transgenic model.

Overall, the relationship between Tau pathology and brain insulin resistance is far from being understood and will deserve further experimental studies. The increased brain insulin response and associated peripheral metabolic alterations of THY-Tau22 Tau transgenic mice described herein, further widens the debate on the role of brain Tau towards insulin signaling and its involvement into the regulation of peripheral metabolism.

Supplementary data to this article can be found online at https://doi.org/10.1016/j.nbd.2019.01.008.

Acknowledgments

This work was supported by grants from France Alzheimer/Fondation de France (InsTauBrain project), FHU VasCog research network (Lille, France) and programs d'investissements d'avenir LabEx (excellence laboratory) DISTALZ (Development of Innovative Strategies for a Transdisciplinary approach to ALZheimer's disease). Our laboratories are also supported by ANR (GRAND, SPREADTAU to LB, ADORATAU & ADORASTrAU to DB), Fondation pour la Recherche Médicale, Vaincre Alzheimer, Fondation Plan Alzheimer as well as Inserm, CNRS, Université Lille, Lille Métropole Communauté Urbaine, Région Hauts-de-France, DN2M. AL and KC hold a doctoral grant from Lille 2 University. EM hold a doctoral grant from CHRU and Région Hauts de France. D. Balschun is supported by Research Foundation - Flanders (FWO).We thank the animal core facility (animal facilities of Université de Lille –Inserm) of « Plateformes en Biologie Santé de Lille » and M Besegher-Dumoulin, J Devassine, Y Lepage, C Meunier, C Degraeve and D Taillieu for transgenic mouse production and care. The authors declare no conflict of interest regarding the present work. We also thanks to Animal experimental platform Chronobiotron of Strasbourg (UMS3415).

References

Benedict, C., De Felice, F.G., 2015. A key role of insulin receptors in memory. Diabetes 64, 3653–3655. https://doi.org/10.2337/dbi15-0011.

Bing, C., Frankish, H.M., Pickavance, L., Wang, Q., Hopkins, D.F., Stock, M.J., Williams, G., 1998 Jan. Hyperphagia in cold-exposed rats is accompanied by decreased plasma leptin but unchanged hypothalamic NPY. Am. J. Phys. 274 (1 Pt 2), R62–R68.

Bloom, S.R., Edwards, A.V., Hardy, R.N., Malinowska, K.W., Silver, M., 1975 Jan. Endocrine responses to insulin hypoglycaemia in the young calf. J. Physiol. 244 (3), 783–803.

Bomfim, T.R., Forny-Germano, L., Sathler, L.B., Brito-Moreira, J., Houzel, J.C., Decker, H., Silverman, M.A., Kazi, H., Melo, H.M., McClean, P.L., Holscher, C., Arnold, S.E., Talbot, K., Klein, W.L., Munoz, D.P., Ferreira, S.T., De Felice, F.G., 2012 Apr. An anti-diabetes agent protects the mouse brain from defective insulin signaling caused by Alzheimer's disease- associated Aβ oligomers. J. Clin. Invest. 122 (4), 1339–1353. https://doi.org/10.1172/JCI57256.

Braak, H., Thal, D.R., Ghebremedhin, E., Del Tredici, K., 2011 Nov. J Neuropathol Exp Neurol 70 (11), 960–969. https://doi.org/10.1097/NEN.0b013e318232a379.

Brown, L.M., Clegg, D.J., Benoit, S.C., Woods, S.C., 2006. Intraventricular insulin and leptin reduce food intake and body weight in C57BL/6J mice. Physiol. Behav. 89, 687–691. https://doi.org/10.1016/j.physbeh.2006.08.008.

Brüning, J.C., Gautam, D., Burks, D.J., Gillette, J., Schubert, M., Orban, P.C., Klein, R., Krone, W., Müller-Wieland, D., Kahn, C.R., 2000. Role of brain insulin receptor in control of body weight and reproduction. Science 289, 2122–2125. https://doi.org/10.1126/science.289.5487.2122.

Burnouf, S., Martire, A., Derisbourg, M., Laurent, C., Belarbi, K., Leboucher, A., Fernandez-Gomez, F.J., Troquier, L., Eddarkaoui, S., Grosjean, M.E., Demeyer, D., Muhr-Tailleux, A., Buisson, A., Sergeant, N., Hamdane, M., Humez, S., Popoli, P., Buée, L., Blum, D., 2013 Feb. NMDA receptor dysfunction contributes to impaired brain-derived neurotrophic factor-induced facilitation of hippocampal synaptic transmission in a Tau transgenic model. Aging Cell 12 (1), 11–23. https://doi.org/10.1111/acel.12018.

Caroni, P., 1997 Jan. Overexpression of growth-associated proteins in the neurons of adult transgenic mice. J. Neurosci. Methods 71 (1), 3–9.

Clarke, J.R., Lyra E Silva, N.M., Figueiredo, C.P., Frozza, R.L., Ledo, J.H., Beckman, D., Katashima, C.K., Razolli, D., Carvalho, B.M., Frazão, R., Silveira, M.A., Ribeiro, F.C., Bomfim, T.R., Neves, F.S., Klein, W.L., Medeiros, R., LaFerla, F.M., Carvalheira, J.B., Saad, M.J., Munoz, D.P., Velloso, L.A., Ferreira, S.T., De Felice, F.G., 2015 Feb. Alzheimer-associated Aβ oligomers impact the central nervous system to induce peripheral metabolic deregulation. EMBO Mol. Med. 7 (2), 190–210. https://doi.org/10.15252/emmm.201404183.

De Felice, F.G., 2013 Feb. Alzheimer's disease and insulin resistance: translating basic science into clinical applications. J. Clin. Invest. 123 (2), 531–539. https://doi.org/10.1172/JCI64595.

de la Monte, S.M., 2014 Dec. Type 3 diabetes is sporadic Alzheimer's disease: mini-review. Eur. Neuropsychopharmacol. 24 (12), 1954–1960. https://doi.org/10.1016/j.euroneuro.2014.06.008.

Duyckaerts, C., Bennecib, M., Grignon, Y., Uchihara, T., He, Y., Piette, F., Hauw, J.J., 1997 May-Jun. Modeling the relation between neurofibrillary tangles and intellectual status. Neurobiol. Aging 18 (3), 267–273.

Gachon, F., Loizides-Mangold, U., Petrenko, V., Dibner, C., 2017 May 1. Glucose homeostasis: regulation by peripheral circadian clocks in rodents and humans. Endocrinology 158 (5), 1074–1084. https://doi.org/10.1210/en.2017-00218.

Gratuze, M., Joly-Amado, A., Vieau, D., Buée, L., Blum, D., 2018. Mutual relationship between Tau and central insulin signalling: consequences for AD and tauopathies? Neuroendocrinology 107 (2), 181–195. https://doi.org/10.1159/000487641.

Grillo, C.A., Tamashiro, K.L., Piroli, G.G., Melhorn, S., Gass, J.T., Newsom, R.J., Reznikov, L.R., Smith, A., Wilson, S.P., Sakai, R.R., Reagan, L.P., 2007 Nov 23. Lentivirus-mediated downregulation of hypothalamic insulin receptor expression. Physiol. Behav. 92 (4), 691–701.

Grillo, C.A., Piroli, G.G., Lawrence, R.C., Wrighten, S.A., Green, A.J., Wilson, S.P., Sakai, R.R., Kelly, S.J., Wilson, M.A., Mott, D.D., Reagan, L.P., 2015 Nov. Hippocampal insulin resistance impairs spatial learning and synaptic plasticity. Diabetes 64 (11), 3927–3936. https://doi.org/10.2337/db15-0596.

Grober, E., Dickson, D., Sliwinski, M.J., Buschke, H., Katz, M., Crystal, H., Lipton, R.B., 1999 Nov-Dec. Memory and mental status correlates of modified Braak staging. Neurobiol. Aging 20 (6), 573–579.

Ishii, M., Wang, G., Racchumi, G., Dyke, J.P., Iadecola, C., 2014 Jul 2. Transgenic mice overexpressing amyloid precursor protein exhibit early metabolic deficits and a pathologically low leptin state associated with hypothalamic dysfunction in arcuate neuropeptide Y neurons. J. Neurosci. 34 (27), 9096–9106. https://doi.org/10.1523/JNEUROSCI.0872-14.2014.

Joly-Amado, A., Serraneau, K.S., Brownlow, M., Marín de Evsikova, C., Speakman, J.R., Gordon, M.N., Morgan, D., 2016 Aug. Metabolic changes over the course of aging in a mouse model of tau deposition. Neurobiol. Aging 44, 62–73. https://doi.org/10.1016/j.neurobiolaging.2016.04.013.

Jucker, M., Walker, L.C., 2013 Sep 5. Self-propagation of pathogenic protein aggregates in neurodegenerative diseases. Nature 501 (7465), 45–51. https://doi.org/10.1038/nature12481.

Kapogiannis, D., Boxer, A., Schwartz, J.B., Abner, E.L., Biragyn, A., Masharani, U., Frassetto, L., Petersen, R.C., Miller, B.L., Goetzl, E.J., 2015 Feb. Dysfunctionally phosphorylated type 1 insulin receptor substrate in neural-derived blood exosomes of preclinical Alzheimer's disease. FASEB J. 29 (2), 589–596. https://doi.org/10.1096/fj.14-262048.

Laurent, C., Burnouf, S., Ferry, B., Batalha, V.L., Coelho, J.E., Baqi, Y., Malik, E., Marciniak, E., Parrot, S., Van der Jeugd, A., Faivre, E., Flaten, V., Ledent, C., D'Hooge, R., Sergeant, N., Hamdane, M., Humez, S., Müller, C.E., Lopes, L.V., Buée, L., Blum, D., 2016 Jan. A2A adenosine receptor deletion is protective in a mouse model of Tauopathy. Mol. Psychiatry 21 (1), 149 (10.1038/mp.2014.151).

Laurent, C., Dorothée, G., Hunot, S., Martin, E., Monnet, Y., Duchamp, M., Dong, Y., Légeron, F.P., Leboucher, A., Burnouf, S., Faivre, E., Carvalho, K., Caillierez, R., Zommer, N., Demeyer, D., Jouy, N., Sazdovitch, V., Schraen-Maschke, S., Delarasse, C., Buée, L., Blum, D., 2017 Jan. Hippocampal T cell infiltration promotes neuroinflammation and cognitive decline in a mouse model of tauopathy. Brain 140 (1), 184–200. https://doi.org/10.1093/brain/aww270.

Leboucher, A., Laurent, C., Fernandez-Gomez, F.J., Burnouf, S., Troquier, L., Eddarkaoui, S., Demeyer, D., Caillierez, R., Zommer, N., Vallez, E., Bantubungi, K., Breton, C., Pigny, P., Buée-Scherrer, V., Staels, B., Hamdane, M., Tailleux, A., Buée, L., Blum, D., 2013 May. Detrimental effects of diet-induced obesity on τ pathology are independent of insulin resistance in τ transgenic mice. Diabetes 62 (5), 1681–1688. https://doi.org/10.2337/db12-0866.

Marciniak, E., Leboucher, A., Caron, E., Ahmed, T., Tailleux, A., Dumont, J., Issad, T.,

Gerhardt, E., Pagesy, P., Vileno, M., Bournonville, C., Hamdane, M., Bantubungi, K., Lancel, S., Demeyer, D., Eddarkaoui, S., Vallez, E., Vieau, D., Humez, S., Faivre, E., Grenier-Boley, B., Outeiro, T.F., Staels, B., Amouyel, P., Balschun, D., Buee, L., Blum, D., 2017 Aug 7. Tau deletion promotes brain insulin resistance. J. Exp. Med. 214 (8), 2257–2269. https://doi.org/10.1084/jem.20161731.

Masters, C.L., Simms, G., Weinman, N.A., Multhaup, G., McDonald, B.L., Beyreuther, K., 1985 Jun. Amyloid plaque core protein in Alzheimer disease and down syndrome. Proc. Natl. Acad. Sci. U. S. A. 82 (12), 4245–4249.

Moloney, A.M., Griffin, R.J., Timmons, S., O'Connor, R., Ravid, R., O'Neill, C., 2010 Feb. Defects in IGF-1 receptor, insulin receptor and IRS-1/2 in Alzheimer's disease indicate possible resistance to IGF-1 and insulin signalling. Neurobiol. Aging 31 (2), 224–243. https://doi.org/10.1016/j.neurobiolaging.2008.04.002.

Mullins, R.J., Mustapic, M., Goetzl, E.J., Kapogiannis, D., 2017 Apr. Exosomal biomarkers of brain insulin resistance associated with regional atrophy in Alzheimer's disease. Hum. Brain Mapp. 38 (4), 1933–1940. https://doi.org/10.1002/hbm.23494.

Nelson, P.T., Alafuzoff, I., Bigio, E.H., Bouras, C., Braak, H., Cairns, N.J., Castellani, R.J., Crain, B.J., Davies, P., Del Tredici, K., Duyckaerts, C., Frosch, M.P., Haroutunian, V., Hof, P.R., Hulette, C.M., Hyman, B.T., Iwatsubo, T., Jellinger, K.A., Jicha, G.A., Kövari, E., Kukull, W.A., Leverenz, J.B., Love, S., Mackenzie, I.R., Mann, D.M., Masliah, E., McKee, A.C., Montine, T.J., Morris, J.C., Schneider, J.A., Sonnen, J.A., Thal, D.R., Trojanowski, J.Q., Troncoso, J.C., Wisniewski, T., Woltjer, R.L., Beach, T.G., 2012 May. Correlation of Alzheimer disease neuropathologic changes with cognitive status: a review of the literature. J. Neuropathol. Exp. Neurol. 71 (5), 362–381. https://doi.org/10.1097/NEN.0b013e31825018f7.

Obici, S., Zhang, B.B., Karkanias, G., Rossetti, L., 2002 Dec. Hypothalamic insulin signaling is required for inhibition of glucose production. Nat. Med. 8 (12), 1376–1382.

Pandini, G., Pace, V., Copani, A., Squatrito, S., Milardi, D., Vigneri, R., 2013 Jan. Insulin has multiple antiamyloidogenic effects on human neuronal cells. Endocrinology 154 (1), 375–387. https://doi.org/10.1210/en.2012-1661.

Randle, P.J., Garland, P.B., Hales, C.N., Newsholme, E.A., 1963 Apr 13. The glucose fatty-acid cycle. Its role in insulin sensitivity and the metabolic disturbances of diabetes mellitus. Lancet 1 (7285), 785–789.

Rodriguez-Rodriguez, P., Sandebring-Matton, A., Merino-Serrais, P., Parrado-Fernandez, C., Rabano, A., Winblad, B., Ávila, J., Ferrer, I., Cedazo-Minguez, A., 2017 Dec 1. Tau hyperphosphorylation induces oligomeric insulin accumulation and insulin resistance in neurons. Brain 140 (12), 3269–3285. https://doi.org/10.1093/brain/awx256.

Schindowski, K., Bretteville, A., Leroy, K., Bégard, S., Brion, J.P., Hamdane, M., Buée, L., 2006 Aug. Alzheimer's disease-like tau neuropathology leads to memory deficits and loss of functional synapses in a novel mutated tau transgenic mouse without any motor deficits. Am. J. Pathol. 169 (2), 599–616.

Sergeant, N., Bretteville, A., Hamdane, M., Caillet-Boudin, M.L., Grognet, P., Bombois, S., Blum, D., Delacourte, A., Pasquier, F., Vanmechelen, E., Schraen-Maschke, S., Buée, L., 2008 Apr. Biochemistry of Tau in Alzheimer's disease and related neurological disorders. Expert Rev. Proteomics. 5 (2), 207–224. https://doi.org/10.1586/14789450.5.2.207.

Sharp, G.W., 1996 Dec. Mechanisms of inhibition of insulin release. Am. J. Phys. 271 (6 Pt 1), C1781–C1799.

Stanley, M., Macauley, S.L., Holtzman, D.M., 2016 Jul 25. Changes in insulin and insulin signaling in Alzheimer's disease: cause or consequence? J. Exp. Med. 213 (8), 1375–1385. https://doi.org/10.1084/jem.20160493.

Steiner, K.E., Stevenson, R.W., Green, D.R., Cherrington, A.D., 1985 Nov. Mechanism of epinephrine's glycogenolytic effect in isolated canine hepatocytes. Metabolism 34 (11), 1020–1023.

Stevanovic, K., Yunus, A., Joly-Amado, A., Gordon, M., Morgan, D., Gulick, D., Gamsby, J., 2017 Aug. Disruption of normal circadian clock function in a mouse model of tauopathy. Exp. Neurol. 294, 58–67. https://doi.org/10.1016/j.expneurol.2017.04.015.

Talbot, K., Wang, H.Y., Kazi, H., Han, L.Y., Bakshi, K.P., Stucky, A., Fuino, R.L., Kawaguchi, K.R., Samoyedny, A.J., Wilson, R.S., Arvanitakis, Z., Schneider, J.A., Wolf, B.A., Bennett, D.A., Trojanowski, J.Q., Arnold, S.E., 2012 Apr. Demonstrated brain insulin resistance in Alzheimer's disease patients is associated with IGF-1 resistance, IRS-1 dysregulation, and cognitive decline. J. Clin. Invest. 122 (4), 1316–1338. https://doi.org/10.1172/JCI59903.

Trayhurn, P., Duncan, J.S., Rayner, D.V., 1995. Acute cold-induced suppression of ob (obese) gene expression in white adipose tissue of mice: mediation by the sympathetic system. Biochem J 311 (3), 729–733 Nov 1.

Troquier, L., Caillierez, R., Burnouf, S., Fernandez-Gomez, F.J., Grosjean, M.E., Zommer, N., Sergeant, N., Schraen-Maschke, S., Blum, D., Buee, L., 2012 May. Targeting phospho-Ser422 by active Tau Immunotherapy in the THYTau22 mouse model: a suitable therapeutic approach. Curr. Alzheimer Res. 9 (4), 397–405.

Van der Heide, L.P., Kamal, A., Artola, A., Gispen, W.H., Ramakers, G.M., 2005 Aug. Insulin modulates hippocampal activity-dependent synaptic plasticity in a N-methyl-d-aspartate receptor and phosphatidyl-inositol-3-kinase-dependent manner. J. Neurochem. 94 (4), 1158–1166.

Van der Jeugd, A., Vermaercke, B., Derisbourg, M., Lo, A.C., Hamdane, M., Blum, D., Buée, L., D'Hooge, R., 2013. Progressive age-related cognitive decline in tau mice. J. Alzheimers Dis. 37 (4), 777–788. https://doi.org/10.3233/JAD-130110.

Vidal, M., Morris, R., Grosveld, F., Spanopoulou, E., 1990 Mar. Tissue-specific control elements of the Thy-1 gene. EMBO J. 9 (3), 833–840.

Wijesekara, N., Konrad, D., Eweida, M., Jefferies, C., Liadis, N., Giacca, A., Crackower, M., Suzuki, A., Mak, T.W., Kahn, C.R., Klip, A., Woo, M., 2005 Feb. Muscle-specific Pten deletion protects against insulin resistance and diabetes. Mol. Cell. Biol. 25 (3), 1135–1145.

Wijesekara, N., Gonçalves, R.A., Ahrens, R., De Felice, F.G., Fraser, P.E., 2018 Jun. Tau ablation in mice leads to pancreatic β cell dysfunction and glucose intolerance. FASEB J. 32 (6), 3166–3173. https://doi.org/10.1096/fj.201701352.

Woods, S.C., Lotter, E.C., McKay, L.D., Porte Jr, D., 1979. Chronic intracerebroventricular infusion of insulin reduces food intake and body weight of baboons. Nature 282, 503–505. https://doi.org/10.1038/282503a0.

Yarchoan, M., Toledo, J.B., Lee, E.B., Arvanitakis, Z., Kazi, H., Han, L.Y., Louneva, N., Lee, V.M., Kim, S.F., Trojanowski, J.Q., Arnold, S.E., 2014 Nov. Abnormal serine phosphorylation of insulin receptor substrate 1 is associated with tau pathology in Alzheimer's disease and tauopathies. Acta Neuropathol. 128 (5), 679–689. https://doi.org/10.1007/s00401-014-1328-5.

Zhao, L., Teter, B., Morihara, T., Lim, G.P., Ambegaokar, S.S., Ubeda, O.J., Frautschy, S.A., Cole, G.M., 2004 Dec 8. Insulin-degrading enzyme as a downstream target of insulin receptor signaling cascade: implications for Alzheimer's disease intervention. J. Neurosci. 24 (49), 11120–11126.

Zhao, N., Liu, C.C., Van Ingelgom, A.J., Martens, Y.A., Linares, C., Knight, J.A., Painter, M.M., Sullivan, P.M., Bu, G., 2017 Sep 27. Apolipoprotein E4 Impairs neuronal insulin signaling by trapping insulin receptor in the endosomes. Neuron 96 (1), 115–129.e5. https://doi.org/10.1016/j.neuron.2017.09.003.